

3D Heat Generation and Transfer in Gravity Dam on Rock Foundation using Galerkin Finite Volume Solver on Tetrahedral Mesh

S.R. Sabbagh-Yazdi and N.E. Mastorakis

Abstract—In order to solve temperature field in a typical gravity concrete dam and its natural foundation, the three-dimensional temperature diffusion equation is chosen as the mathematical model. The finite volume formulation is derived using Galerkin approach for the mesh of tetrahedral elements. This method facilitates solving temperature problems with complicated geometries. The algorithm not only is able to handle the essential boundary conditions but also the natural boundary conditions using a novel technique. Accuracy and efficiency of the algorithm is assessed by comparison of the numerical results for a bench mark problem of heat generation and transfer in a block with its analytical solution. Finally the developed model is applied to compute temperature field in a three dimensional gravity concrete dam on rock foundation.

Keywords—Heat Transfer in Rock and Concrete, Galerkin Finite Volume Solution, Tetrahedral Computational Mesh

I. INTRODUCTION

Temperature profiles in the concrete gravity dams (as mass concrete structures) and their rock foundation form due to the heat generation sourcing from cement hydration. The temperature profiles depend to the heat exchange with the surrounding ambient result in time varying temperature profiles in the structure. On the other hand, tensile stresses develop in the structure due to restrained thermal movements. Leaving unchecked such an effect can result in thermal cracking of the concrete. Hence, thermal considerations are critical tasks in concrete gravity dams. This fact makes temperature profile simulation an important part of the design and construction process.

Availability of the fast and powerful personal computers motivates the use of numerical methods for solving temperature fields of engineering applications. In order to predict the thermal behavior of the solid states with internal source of heat generation rate several numerical solvers are developed using various methods such as Finite Difference Methods, Finite Element Methods and Finite Volume

Methods. The Finite Differences [1] convert differential form of the governing equations to simple formulations in the expense of some errors which degrades the accuracy of the numerical solutions. But the main problem of the Finite Difference Methods is serious difficulties in their application to solve real world problems due to necessity of the use of structured grids for geometric discretization.

The Finite Element Method [2] and Boundary Element Method [3] overcome the aforementioned problem by application of sophisticated mathematical manipulations on the integral form of the governing equations formulations which end up with complicated solution procedures. Consequently, the Finite Element Methods not only can handle complex geometries but also provide accurate numerical solutions for the boundary value problems. However, their heavy computational work load, time-consuming complicated matrix computations and implicit solutions of real world applications with geometrical complexities some times are beyond the available hard ware efficiencies.

The traditional Finite Volume Methods [4] convert the integral form of the governing equations for spatial problems into simple algebraic formulations. These methods may have some advantages over the Finite Difference Methods but the required structured meshes bring up major restrictions and errors with modeling of domains with complex geometries and irregular boundaries. The Finite Volume Methods suitable for the unstructured meshes [5] can handle the geometrical complexities using relatively simple formulations and computational procedures. Therefore, if the developed algorithm of these types of Finite Volume Method can satisfy the accuracy requirements of the desired problem, it would be an efficient means of computer simulations of the engineering applications on ordinary hard ware systems.

Following the previous work of the first author [6] and [7], a numerical solution algorithm for the temperature field under the effects of internal heat generation rate as well as essential and natural boundary conditions is described. Here, the Galerkin finite volume solution algorithm is described and used for temporal solution of diffusive equation of heat generation and transfer. For this purpose, the governing equation of heat generation and transfer is multiplied by the piece wise linear shape function of tetrahedral elements of an

Manuscript received April 2, 2007; Revised version received October 19, 2007

Saeed-Reza Sabbagh-Yazdi is Associate Professor Civil Engineering Department of K.N. Toosi University of Technology, 1346 Valiasr St. Tehran, IRAN (phone: +9821-88521-644; fax: +9821-8877-9476; e-mail: SYazdi@kntu.ac.ir).

Nikos E. Mastorakis is Professor of Military Institutes of University Education (ASED), Hellenic Naval Academy, Terma Chatzikyriakou 18539, Piraeus, GREECE.

unstructured mesh and then it is integrated over all control volumes formed by the elements meeting every computational node (vertices of the elements). The algorithm takes advantage from the fact that the first derivatives of the linear interpolation function for the temperature are constant inside each element. By application of Gauss divergence theorem and using the property of the linear shape function, which satisfies homogeneous boundary condition on the dependent variable, the boundary integral terms can be omitted for every control volumes using surrounding nodal values. After some manipulations, the resulting formulations can be solved explicitly with rather light computational efforts.

Using a novel numerical technique for imposing natural boundary conditions on incline boundaries are used for reducing computational efforts. Hence, an efficient solver is developed for the solution of three-dimensional temperature fields with complex boundaries which geometrically can be modeled by the use of unstructured mesh of tetrahedral elements. In order to assess the performance of the developed solver, the numerical solution results of temperature in a typical block are compared with its analytical solution. Finally the developed model is applied to compute temperature field in a three dimensional monolith of a gravity concrete dam with upstream and downstream slopes located on natural rock foundation.

II. MATHEMATICAL MODEL

A. Differential Form

Assuming isotropic thermal properties for the solid materials, the familiar equation defining heat generation and transfer is of the form,

$$\alpha \left(\frac{\partial^2 T}{\partial x_i^2} \right) + \frac{\alpha}{\kappa} \dot{Q} = \frac{\partial T}{\partial t} \quad (i=1,2,3) \quad (1)$$

Here, T ($^{\circ}C$) and \dot{Q} (KJ/m^3h) are temperature and the rate of heat generation per unit volume, respectively. If thermal diffusion is defined as $\alpha = \kappa / \rho C$, where the parameters are ρ (Kg/m^3) density, C ($KJ/Kg^{\circ}C$) specific heat, κ ($W/m^{\circ}C$) heat conduction coefficient, respectively.

Consider the governing equation for heat generation and transfer in a homogenous domain as,

$$\frac{\partial T}{\partial t} + \frac{\partial}{\partial x_i} \left(\alpha \frac{\partial T}{\partial x_i} \right) = S \quad (i=1,2,3) \quad (2)$$

Where T (temperature) is the unknown parameter and $S = \alpha \dot{Q}(t_e) / \kappa$ is the heat source. If temperature gradient fluxes in i direction (secondary variable) are defined as,

$$F_i^d = \alpha \frac{\partial T}{\partial x_i} \quad (i=1,2,3) \quad (3)$$

And hence, the equation takes the form:

$$\frac{\partial T}{\partial t} + \left(\frac{\partial}{\partial x_i} F_i^d \right) = S \quad (i=1,2,3) \quad (4)$$

A. Definition of Boundary Conditions

The natural boundary condition for the equation on concrete external surface is taken as,

$$\kappa \left(\frac{\partial T}{\partial x_i} n_i \right) + q = 0 \quad (i=1,2,3) \quad (5)$$

Where, q is the rate of heat exchange per unit volume of concrete surface with surrounding ambient and the vector $\hat{n} = n_1 \hat{i} + n_2 \hat{j} + n_3 \hat{k}$ is the surface boundary normal. The rate of heat exchange q is taken into consideration through three mechanisms, q_c (convection), q_r (long wave radiation of concrete to surroundings) and q_s (solar radiation absorption). Hence, the total rate of heat exchange can be defined as, $q = \pm q_c + q_r - q_s$ [8].

B. Definition of Source Term

In order to compute the source of the heat generation rate in the concrete body, \dot{Q} , the considerable influence of the temperature on hydration rate of cementation materials should be properly considered. For this propose, due to effects of ambient temperature on the rate of heat generation of cements, it is necessary to take the temperature history of various points in concrete body into account.

The heat generation rate can be expressed in terms of equivalent time $t_e = \int H(T) dt$ as,

$$\dot{Q}(t_e) = \left(\frac{dQ(t_e)}{d(t_e)} \right) \left(\frac{d(t_e)}{dt} \right) \quad (6.a)$$

Due to the considerable influence of the temperature on hydration rate of cementation materials, it is necessary to take the temperature history of various points in concrete body into account. Various functions have been proposed for considering this effect and are referred to as maturity function [9]. The function proposed by Rastrup [10] is a well-known example. The time derivative of equivalent time is determined using the relative rate of reaction concept as:

$$\frac{d(t_e)}{dt} = H(T) = 2^{0.1(T-T_r)} \quad (6.b)$$

where T_r is a reference temperature. Using heat evolution of concrete as a function of equivalent time $Q(t_e)$ [9], we have

$$\frac{dQ(t_e)}{d(t_e)} = nbE[t_e]^{-n-1} \exp\{-b[t_e]^{-n}\} \quad (6.c)$$

Where, E , b and n are constants obtained by regression of experimental heat evolution data.

Note that using the expressions (6.b) and (6.c), for every single point of the concrete body, the rate of heat generation \dot{Q} can be computed by equation (6.a) considering as a function of equivalent time t_e by using a reference temperature T_r and taking the temperature history into account.

III. NUMERICAL MODEL

A. Galerkin Finite Volume Formulation

Following the concept of weighted residual methods, by considering the test function equal to the weighting function, the dependent variable inside the domain Ω can be approximated by application of a linear combination, such as $T = \sum_{k=1}^{N_{nodes}} T_k \varphi_k$ [7].

According to the Galerkin method, the weighting function ϕ can be chosen equal to the interpolation function, φ . In finite element methods this function is systematically computed for desired element type and called the shape function. For a tetrahedral element (with four nodes), the linear shape functions, φ_k , takes the value of unity at desired node n , and zero at other neighboring nodes k of each triangular element ($k \neq n$) [7].

Extending the concept to a sub-domain to the control volume formed by the elements meeting node n (Figure 1), the interpolation function φ_n takes the value of unity at the center node n of control volume Ω and zero at other neighboring nodes m (at the boundary of the control volume Γ). Noteworthy that, this is an essential property of weight function, φ , which should satisfy homogeneous boundary condition on T at boundary of sub-domain [3]. That is why the integration of the linear combination $T = \sum_{k=1}^{N_{nodes}} T_k \varphi_k$ (as approximation) over elements of sub-domain Ω takes the value of T_n (the value of the dependent variable in central node n). By this property of the shape function φ ($\varphi_n = 0$ on boundary Γ of the sub-domain Ω), the boundary integral term in equation (9) takes zero value for a control volume which the values of T assumed known at boundary nodes.

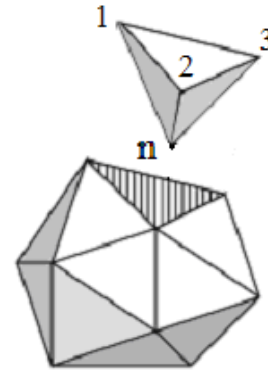


Figure 1 - Sub-domain Ω associated with node n of

By application of the Variational Method [11], after multiplying the residual of the above equation by the test function ϕ and integrating by parts over a sub-domain Ω , application of Gauss divergence theorem and omitting zero term, the equation (4) takes the form,

$$\frac{\partial}{\partial t} \int_{\Omega} T \varphi \, d\Omega \quad (i=1,2,3) \quad (7)$$

$$- \int_{\Omega} F_i^d \frac{\partial \varphi}{\partial x_i} \, d\Omega = \int_{\Omega} S \varphi \, d\Omega$$

In order to drive the algebraic formulation, every single term of the above equation first is manipulated for each element then the integration over the control volume is performed. The resulting formulation is valid for the central node of the control volume.

For the terms containing no derivatives of the shape function φ , an exact integration formula is used as $\int_{\Lambda} \varphi_1^a \varphi_2^b \varphi_3^c \varphi_4^d = 6\Lambda (a!b!c!d!)/(a+b+c+d+3) = \Lambda/4$ (for $a=1$ and $b=c=d=0$), where Λ is the volume of the tetrahedral element [12]. This volume can be computed by the integration formula as,

$\Lambda = \int_{\Lambda} x_i (d\Lambda)_i \approx \sum_k^4 [\bar{x}_i \delta \ell_i]_k$ where \bar{x}_i and $\delta \ell_i$ are the average i direction coordinates and projected area (normal to i direction) for every side face opposite to node k of the element.

Therefore, the transient term $\frac{\partial}{\partial t} \int_{\Omega} \phi T \, d\Omega$ for each tetrahedral element Λ (inside the sub-domain) can be written as, $\frac{\partial}{\partial t} \int_{\Lambda} \phi T \, d\Lambda = (\Lambda/4) \frac{dT}{dt}$. Consequently, the transient term of equation (10) for the sub-domain Ω (with central node n) takes the form,

$$\frac{\partial}{\partial t} \int_{\Omega} \varphi T \, d\Omega = \frac{\Omega_n}{4} \frac{dT_n}{dt} \quad (8.a)$$

Similarly, the source term of equation (7), $\int_{\Omega} S \varphi d\Omega$, for each element Λ (inside the sub-domain), will be written as, $\int_{\Lambda} \varphi S d\Lambda = (\Lambda/4) S$. Then the source term of the equation (10), for the control volume Ω (with central node n) takes the form,

$$\int_{\Omega} \varphi S d\Omega = \frac{\Omega_n}{4} S_n \quad (8.b)$$

Now we try to discretize the terms containing spatial derivative, $\int_{\Omega} F_i^d (\partial\phi/\partial x_i) d\Omega$. Since the only unknown dependent variable is $T = \sum_k^4 T_k \varphi_k$ and the shape functions, φ_k , are chosen piece wise linear in every tetrahedral element, the temperature gradient flux (F_i^d is formed by first derivative) is constant over each element and can be taken out of the integration. On the other hand, the integration of the shape function spatial derivation over tetrahedral element can be converted to boundary integral using Gauss divergence theorem [9], and hence, $\int_{\Lambda} \partial\varphi/\partial x_i d\Lambda = -\oint_{\Delta} \varphi(d\Delta)_i$. Here Δ is component of the side face element normal to the i direction. The discrete form of the line integral can be written as, $\oint_{\Delta} \varphi(d\Delta)_i \approx 1/\Lambda \sum_k^4 [\bar{\varphi} \delta\ell_i]_k$, where $[\bar{\varphi} \delta\ell_i]_k$ is formed by considering the side of the element opposite to the node k , and then, multiplication of its component perpendicular to the i direction by $\bar{\varphi}$ the average shape function value of its three end nodes. Hence, the term $\int_{\Omega} F_i^d (\partial\phi/\partial x_i) d\Omega \approx -\sum_n^N [F_i^d/\Lambda \sum_k^4 (\bar{\varphi} \delta\ell_i)_k]$ for a control volume Ω (containing N elements sharing its central node). Since the shape function φ takes the value of unity only at central node of control volume and is zero at the nodes located at the boundary of control volume, $\bar{\varphi} = 1/3$ for the faces connected to the central node of control volume and $\bar{\varphi} = 0$ for the boundary faces of the control volume. On the other hand the sum of the projected area (normal to i direction) of three side faces of every tetrahedral element equates to the projected area of the fourth side face, hence the term containing spatial derivatives in i direction of the equation (7), can be written as,

$$\int_{\Omega} F_i^d \frac{\partial\varphi}{\partial x_i} d\Omega = -\frac{1}{3} \sum_{m=1}^M [F_i^d \delta\ell_i]_m \quad (11.c)$$

Where $[\delta\ell_i]_m$ is the component of the boundary face m (opposite to the central node of the control volume Ω)

perpendicular to i direction. Note that, F_i^d is computed at the center of tetrahedral element of the control volume, which is associated with side m . The temperature gradient flux in i direction, $F_i^d = \alpha \partial T / \partial x_i$, at each tetrahedral element can be calculated using Gauss divergence theorem, $\int_{\Omega} F_i^d d\Omega = \alpha \int_{\Lambda} \partial T / \partial x_i d\Lambda = -\alpha \oint_{\Delta} T (d\Delta)_i$, where $(d\Delta)_i$ is the projection of side faces of the element perpendicular to i direction. By expressing the boundary integral in discrete form as, $\oint_{\Delta} T (d\Delta)_i \approx \sum_k^3 (\bar{T} \delta\ell_i)_k$, for each element inside the control volume Ω . Therefore, we have,

$$[F_i^d]_m = -\frac{1}{\Lambda_m} \sum_{k=1}^3 (\bar{T} \delta\ell_i)_k \quad (9)$$

Where, $\delta\ell_i$ is the component of k^{th} face of a tetrahedral element (perpendicular to the i direction) and \bar{T} is the average temperature of that face and Λ is the volume of the element.

Note worthy that for control volumes at the boundary of the computational domain, central node n of the control volume Ω locates at its own boundary. For the boundary sides connected to the node n there are no neighboring element to cancel the contribution. Hence, their contributions remain and they act as the boundary sides of the sub-domain. Therefore, there is no change to the described procedure for computation of the spatial derivative terms $\int_{\Omega} F_i^d (\partial\varphi/\partial x_i) d\Omega$.

Finally, using expressions (8.a), (8.b) and (8.c), the equation (7) can be written for a control volume Ω (with center node n) as:

$$\Omega_n \frac{dT_n}{dt} = \Omega_n S_n - \frac{4}{3} \sum_{m=1}^M [F_i^d \delta\ell_i]_m \quad (i=1,2,3) \quad (10)$$

The volume of control volume, Ω can be computed by summation of the volume of the elements associated with node n .

Remember, the heat source for each node n in concrete body is defined by $S_n = \alpha_n \dot{Q}(t_e)_n / \kappa_n$.

The resulted numerical model, which is similar to Non-Overlapping Scheme of the Cell-Vertex Finite Volume Method on unstructured meshes, can explicitly be solved for every node n (the center of the sub-domain Ω which is formed by gathering elements sharing node n). The explicit solution of temperature at every node of the domain of interest can be modeled as,

$$T_n^{t+\Delta t} = T_n^t + \delta t \left[S_n - \frac{3}{2\Omega_n} \left(\sum_{k=1}^N F_i^d \Delta\ell_i \right)_n \right] \quad (i=1,2) \quad (11)$$

B. Time Integration

Now we need to define a limit for the explicit time step, δt . Considering thermal diffusivity as $\alpha = \kappa / \rho C$ with the unit (m^2/s), the criterion for measuring the ability of a material for temperature change. Hence the rate of temperature change can be expressed as, $\Omega_n / \delta t \approx \alpha_n$. Therefore, the appropriate size for local time stepping can be considered as,

$$\delta t = \beta \frac{\Omega_n}{\alpha_n} \quad (\beta \leq 1) \quad (12)$$

β is considered as a proportionality constant coefficient, which its magnitude is less than unity. For the steady state problems this limit can be viewed as the limit of local computational step toward steady state.

However, there are different sizes of control volumes in unstructured meshes. This fact implies that the minimum magnitude of the above relation be considered. Hence, to maintain the stability of the explicit time stepping the global minimum time step of the computational field should be considered, so,

$$\delta t = \beta \left(\frac{\Omega_n}{\alpha_n} \right)_{\min} \quad (\beta \leq 1) \quad (13)$$

Noteworthy that for the solution of steady state problems on suitable fine unstructured meshes, the use of local computational step instead of global minimum time step may considerably reduce the computational efforts.

C. Implementation of Boundary Conditions

Two types of boundary conditions are usually applied in this numerical modeling. The essential and natural boundary conditions are used for temperature and temperature gradient flux (gradients) at boundaries, respectively [7].

For those boundary nodes where nodal temperatures are to be imposed (essential boundary conditions), there is no need to compute the temperature. Hence, computed temperature at those node have to be replaced by the given certain values at the end of each computational step.

Contrarily, there is no need to change the computed temperature at the boundary nodes where the natural boundary condition is to be imposed. In order to impose a given temperature gradient normal to the boundary faces, G (the rate of heat exchange per unit volume of the surface), the normal vector of the boundary faces $\bar{n}_m = (n_{m1}, n_{m2}, n_{m3})$ can be utilized to compute $\bar{G} = (Gn_{m1}, Gn_{m2}, Gn_{m3})$ at the desired boundaries. Although simple techniques for imposing gradient at boundary can be applied for the cases that the boundary normal is parallel to one of the main directions of coordinate system, computational difficulties arise for the

inclined or curved boundaries. For overcoming the problem, the computed gradient flux vector, $\bar{F}^d = (F_1^d, F_2^d, F_3^d)$, at the centre of adjacent element may be modified at the end of each computational step. First, the vector of temperature gradient tangent to the desired boundary face is decomposed from the computed gradient at the centre of adjacent element,

$$\bar{F}_{Tangential} = \bar{G} - (\bar{F}^d \cdot \bar{n}_m) \bar{n}_m \quad (14.a)$$

Then, the normal vector of temperature gradient can be imposed as,

$$\bar{F}_{Normal} = |\bar{G}| \bar{n}_m \quad (14.b)$$

Finally, the temperature gradient vector at the centre of element adjacent to the desired boundary face is considered as,

$$\bar{F}_{Modified}^d = \bar{F}_{Tangential} + \bar{F}_{Normal} \quad (15)$$

Using above mention technique the difficulties associated with inclined or curve boundaries are overcome. Therefore, the proposed technique suites the present algorithm which is adopted for the domains with complex boundaries discretized using unstructured meshes.

IV. MESH GENERATION

Structured tetrahedral mesh can be generated by considering 5 or 6 tetrahedron between an eight noded cubic mesh spacing (Figure 2). A general view of two typical meshes which are formed by considering 5 or 6 tetrahedron between an eight noded cubic mesh spacing are presented in figure 3.

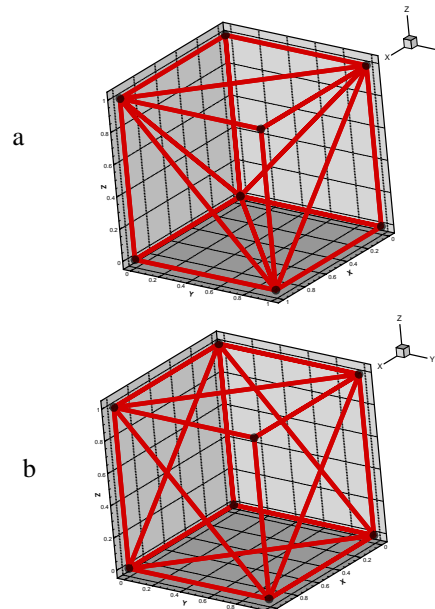


Fig. 2 Two cubic mesh spacing formed by eight nodes which are filled by a) 5 and b) 6 tetrahedral

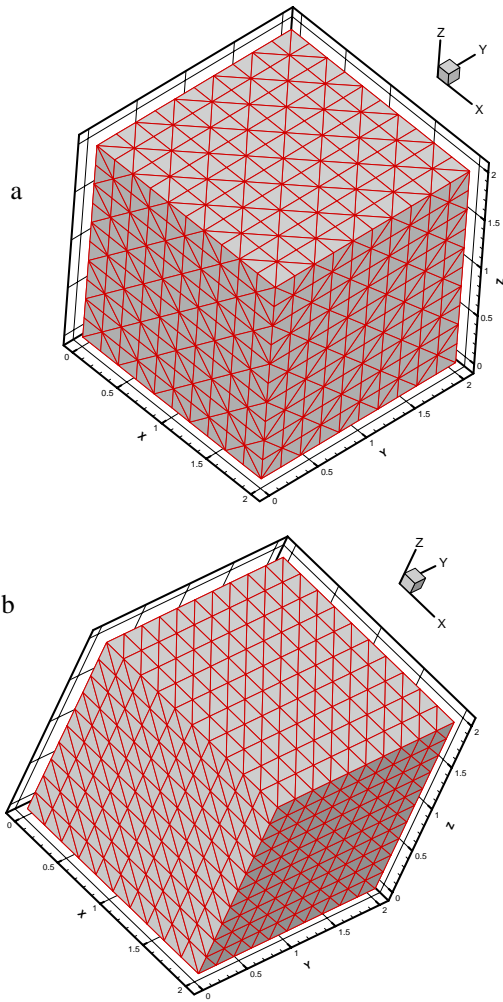


Fig. 3 A general view of two typical meshes which are formed by considering 5 or 6 tetrahedron between an eight node cubic mesh spacing.

V. VERIFICATION CASES

A. Heat Generation and Transfer in a Cub

The accuracy of the solution of spatial derivative terms is investigated by comparison of the results of the numerical solver with the analytical solution of the following steady state diffusion equation (boundary value problem) with a constant source term as [2],

$$k \frac{\partial^2 T}{\partial x_i^2} = Q_0 \quad (i = 1,2) \quad (16)$$

in the spatial field of $\Omega = \{0 < (x, y) < 1\}$. Considering the constants of the above equation as $k = 1$ and $Q_0 = 1$ as well as the boundary conditions at $x = 1, y = 1$ as $T = 0$

and $\frac{\partial T}{\partial n} = 0$ at $x_1 = 0, x_2 = 0$. The analytical solution is given by [2],

$$T(x, y) = \frac{1}{2} \left\{ (1 - y^2) + \frac{32}{\pi^3} \sum_{n=1}^{\infty} \frac{(-1)^n \cos[(2n-1)\pi y / 2] \cosh[(2n-1)\pi x / 2]}{(2n-1)^3 \cosh[(2n-1)\pi / 2]} \right\} \quad (17)$$

In order to obtain a temperature field similar to the two dimensional solution of this problem on a section of the cube, the requirement of imposing natural boundary condition is relaxed by doubling the dimension, and hence, essential boundary condition ($T = 0$) is imposed over four the boundaries $\{(x, y) = -1, 1\}$ and natural boundary condition ($\frac{\partial T}{\partial n} = 0$) at $\{(z) = -1, 1\}$. The tetrahedral mesh which is generated by considering 6 tetrahedral between cubic mesh spacing with eight nodes is presented in figure 3.b. This $2m \times 2m$ mesh is formed by $11 \times 11 \times 11$ grid points.

The result of the numerical solution of equation (16) is shown in figure 4 in the form of temperature contour maps. The accuracy of numerical solution can be assessed in figures 5 by comparison between the computational and the analytical solution in two directions along the two lines in the cub.

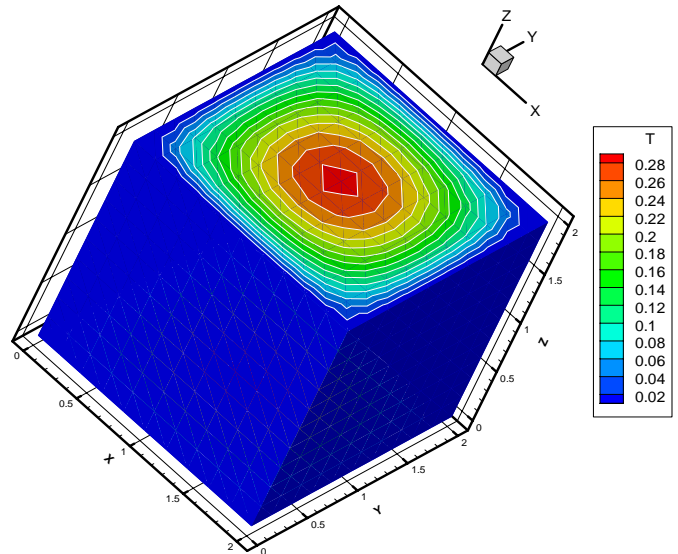


Fig. 4 Computed temperature field in a cubic

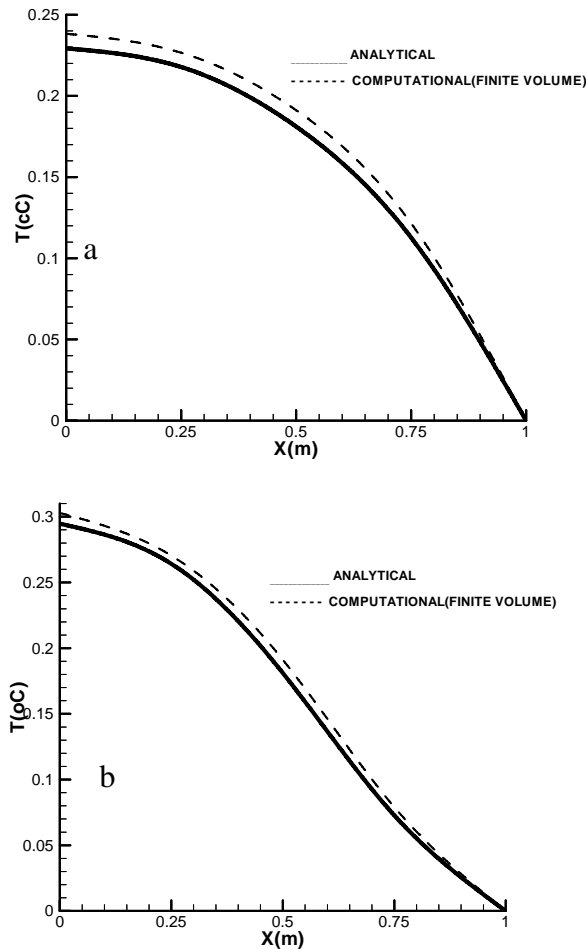


Fig. 5 Comparison between the computational and the analytical solution,
 a: along the line $y=0$ ($0 < x < 1$) and
 b: along the line $y=x$ ($0 < x < 1$)

B. Heat Generation and Transfer in Prisms

In order to assess the performance of introduced technique for imposing natural boundary conditions (i.e. symmetric condition $\frac{\partial T}{\partial n} = 0$) at incline boundary surfaces a reduction is considered on computational field of previous test case. This is done by dividing the original field into a prism that its volume is equal to 1/16 of original test case (figure 6). As can be seen one of the symmetry surfaces is incline.

The computed temperature fields which are computed using natural boundary conditions on symmetry boundaries of the mesh is presented at figure 6 are shown in figure 7 in the form of color coded map of temperature field. As can be seen the applied technique for imposing natural boundary condition preserves the accuracy of temperature gradients, even on inclined surfaces.

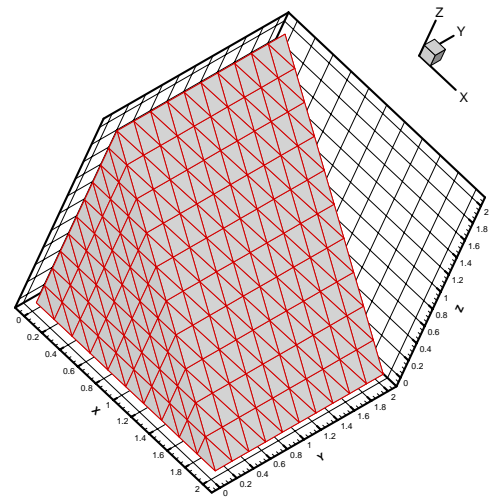


Fig. 6. 3D mesh of a prism with an incline boundary surface

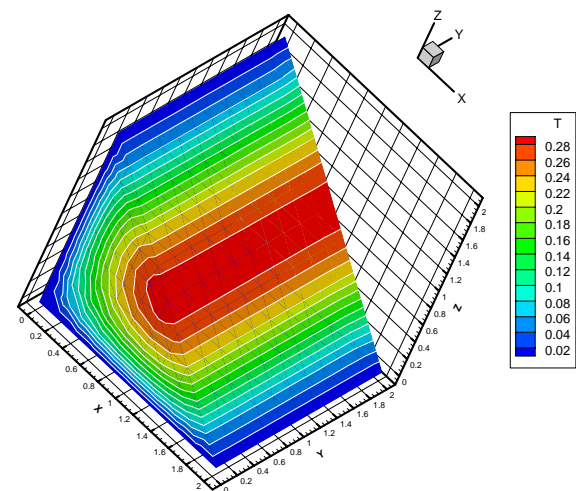


Fig. 7. Computed color coded map of temperature field in a prism with an incline boundary surface

C. Cement Heat Generation in a Concrete Cub

In order to evaluate the accuracy of the source term representing the rate of the heat generation, a set of experimental measurements on a concrete cube with $100 \times 100 \times 120$ (cm³) dimensions cast by 300 kg/m^3 is used [10]. The concrete block was insulated all over the faces and is placed in the shade, therefore radiation and sun did not considered in the modeling. The convection from the isolation is considered by considering a sinusoidal variation of ambient temperature

between 19.5 and 24.5 °C. The coefficients of the described relation for the heat generation are calibrated for the applied cement and tabulated in the reference. A three dimensional rectangular triangular mesh with 2.5 cm spacing is utilized for numerical simulations. Assuming the concrete was kept in shaded area, the effect of solar radiations was omitted. The properties of concrete is considered as $\alpha_c = 0.0038 \text{ m}^2/\text{h}$ and $\kappa = 9 \text{ KJ/m}^3 \text{ ch}$. The average experimental data have been measured at some points of concrete block.

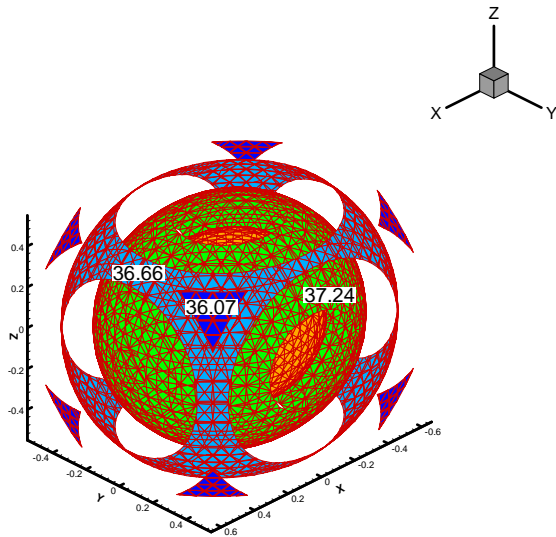


Fig.8. Computed temperature profiles in terms of iso-temperature surfaces

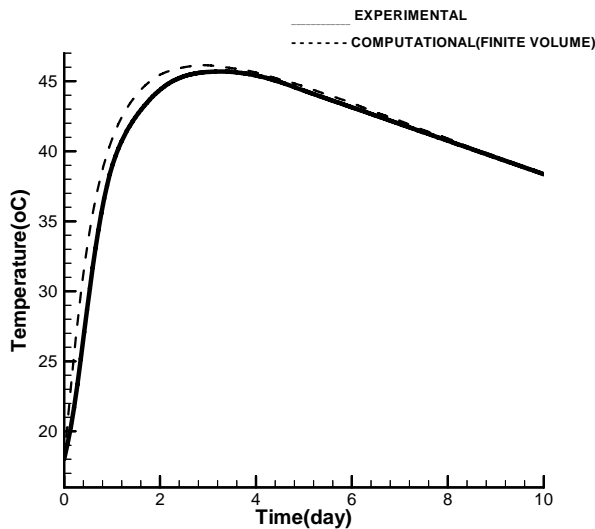


Fig.9. Comparison of computed results with the experimental data for a permanently isolated concrete block

The computed temperature profiles in terms of color coded temperature surfaces are plotted in figure 8. The results of the computer model are compared with the experimental data for the permanently isolated concrete block present reasonable agreements, in figure 9.

I. APPLICATION CASE

In this section, the application of the developed three-dimensional Galerkin finite volume solver is demonstrated. For this purpose, the developed model is applied to compute temperature field in a three dimensional monolith of a gravity concrete dam with 10 m, height 10 m base, 0.1:1 upstream and 0.8:1 downstream slopes located on a 15×15 ×15 (m³) natural rock foundation (Figure 10).

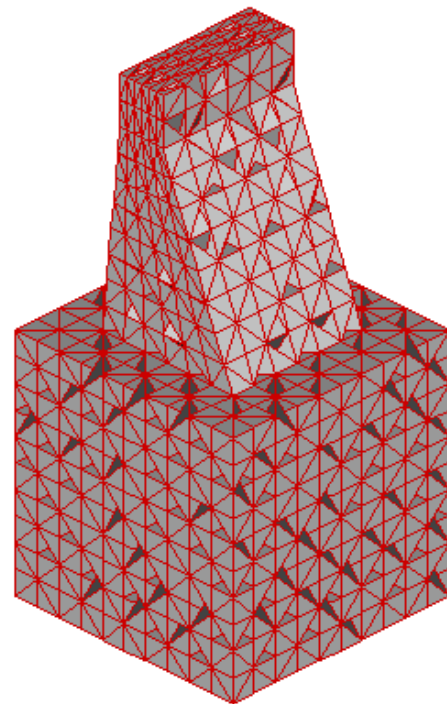


Fig.10. Computational model for a gravity concrete dam monolith on rock foundation

The cement content of the concrete is considered to be 150 kg/m³. The convection from the gravity concrete monolith dam surfaces is considered by considering a sinusoidal variation of ambient temperature between 14 and 26^o C. It is assumed that the vertical is of the monolith covered by e=5 cm form work on The coefficients of the described relation for the heat generation are calibrated for the applied cement and tabulated in the reference. The properties of concrete is considered as $\alpha_c = 0.0038$ (m²/h) and $\kappa = 9$ (KJ / m^och). The average experimental data have been measured at some points of concrete block. The rock foundation is assumed to be sand granite.

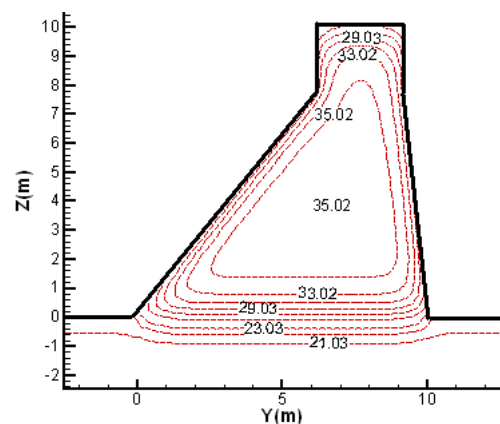


Fig.11. Computed color coded temperature lines at the final stage of dam completion in a vertical section

The laminar construction of the concrete part of the computational domain is modeled by gradual activation of the horizontal layers of the structured mesh. The computed

temperature profiles at the final stage of dam completion are plotted in terms of color coded temperature lines in a vertical section in figure 11. The maximum computed temperatures during the construction of the dam are plotted in figure 12.

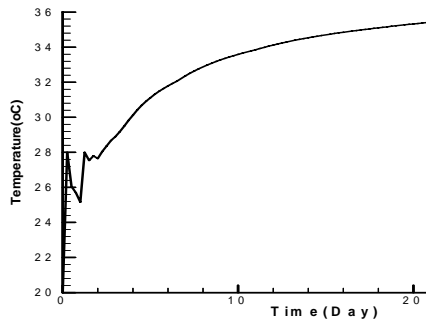


Fig.12. Computed maximum temperature during dam completion

II. CONCLUSION

The equation of heat generation and transfer is solved on triangular element mesh utilizing linear shape function as an alternative test function. The resulted Galerkin finite volume algorithm provides light explicit computation of time dependent problems.

The numerical model was verified in three stages. First, by using a boundary value problem and its analytical solution, the accuracy of the solution of the spatial terms was assessed. Second, the quality of the results for imposing natural boundary conditions on incline surfaces is assessed. Third, adopted formulation for source term of heat generation rate of the concrete is evaluated by the comparison of the computed results with the available experimental measurements.

The results of the developed model present reasonable agreements to the analytical and experimental data.

The direction of edges did not degrade the computational results and no worse effect due to unidirectional edges inside the mesh was appeared in the solution results.

Application of the developed model for a multi material case with complicated boundary surfaces is examined by modeling temperature field in a three dimensional monolith of a gravity concrete dam with upstream and downstream slopes located on natural rock foundation.

The efficiency of the present modeling algorithm and the accuracy of the results encourage its further developments and application to the real world problems.

REFERENCES

- [1] D.A. Anderson, J.C. Tannehill, R.H. Pletcher, "Computational Fluid Mechanics and Heat Transfer", Cambridge Hemisphere Press, 1984.
- [2] J.N. Reddy and D.K. Gartling, "The Finite Element Method in Heat Transfer and Fluid Dynamics", CRC Press, 2000.
- [3] C.A. Bercia, J.C.F. Telles, L.C. Wrobel, "Boundary Element Technique Theory and Application in Engineering", Springer Verlag, Berlin, 1984
- [4] S.V. Patankar, "Numerical Heat Transfer and Fluid Flow", McGraw Hill, 1980.

- [5] J.F. Thompson, B.K. Soni and N.P. Weatherill, *Hand book of grid generation*, CRC Press, New York, 1999.
- [6] S.R. Sabbagh-Yazdi, N.E. Mastorakis and A.R. Bagheri "Galerkin Finite Volume Solution of Heat Generation and Transfer in RCC Dams" *International Journal of Mathematical Models and Methods in Applied Sciences*, Issue 4, Vol.1, 2007, pp. 261-268.
- [7] S.R. Sabbagh-Yazdi and E.N. Mastorakis, "Efficient Symmetric Boundary Condition for Galerkin Finite Volume Solution of 3D Temperature Field on Tetrahedral Meshes", *5th IASME / WSEAS International Conference on Heat Transfer, Thermal Engineering and Environment*, Vouliagmeni Beach, Greece, 2007.
- [8] E.L. Wilson, "The Determination of Temperatures Within Mass Concrete Structure", Report No. 68-17, Department of Civil Eng., University of California, Berkeley, 1968.
- [9] S.R. Sabbagh-Yazdi, A.R. Bageri "Computer Simulation of Cement Heat Generation and Temperature Profiles in Mass Concrete Structures", *IUST International Journal of Engineering Science*, No.2, Vol.15, spring 2004.
- [10] F.A. Branco, P.A. Mendes, E. Mirambell, "Heat of Hydration Effects in Concrete Structures", *ACI Materials Journal*, 1992, pp. 139-145.
- [11] J.N. Reddy, "An Introduction to the Finite Element Method", McGraw-Hill, Mathematics and Statistics Series, 2005.
- [12] O.C. Zienkiewicz and R.L Taylor., "The Finite Element Method, Volume 1 Basic Formulation and Linear Problems", McGraw-Hill, 1988

First Author's biography may be found in:
<http://sahand.kntu.ac.ir/~syazdi/>